Journal of Hazardous Materials 213–214 (2012) 93–99

Contents lists available at SciVerse ScienceDirect

Journal of Hazardous Materials

journal homepage: www.elsevier.com/locate/jhazmat

Transport and interactions of kaolinite and mercury in saturated sand media

Yingjia Zhu[a], Lena Q. Ma[a,*], Bin Gao[b], J.C. Bonzongo[c], Willie Harris[a], Binhe Gu[d]

[a] Soil and Water Science Department, University of Florida, Gainesville, FL 32611, United States
[b] Department of Agricultural and Biological Engineering, University of Florida, Gainesville, FL 32611, United States
[c] Department of Environmental Engineer and Sciences, University of Florida, Gainesville, FL 32611, United States
[d] South Florida Water Management District, West Palm Beach, FL 33411, United States

ARTICLE INFO

Article history:
Received 4 August 2011
Received in revised form 13 October 2011
Accepted 19 January 2012
Available online 28 January 2012

Keywords:
Kaolinite
Colloid-facilitated transport
Column experiment
Hg
Modeling

ABSTRACT

To evaluate the potential of Hg release and co-transport by colloids, it is important to understand how Hg, colloids and Hg-loaded colloids migrate in soils. Hg sorption by kaolinite and sand were nonlinear and fit the Langmuir model, with the maximum Hg sorption capacity being 1.2 mg/g kaolinite and 0.11 mg/g sand. Co-transport of Hg and kaolinite was evaluated using: (1) 1 or 100 mg/L Hg or 100 mg/L kaolinite, (2) 1 or 100 mg/L Hg mixed with 100 mg/L kaolinite, (3) 1 or 100 mg/L Hg presorbed onto kaolinite, and (4) 250 mg/L kaolinite in Hg-loaded sand columns. The presence of kaolinite (100 mg/L) reduced Hg's mobility through sand column by increasing deposition rate of Hg-loaded kaolinite. At 100 mg/L Hg, soluble Hg dominated Hg transport; but at 1 mg/L Hg, colloidal Hg (Hg sorbed on kaolinite) affected Hg transport. Preloading 100 mg/L Hg onto kaolinite (0.43 mg/g) reduced kaolinite's mobility with low recovery rate (78%), with Hg retardation ($R = 1$) in Hg-loaded kaolinite being lower than Hg retardation at 100 mg/L Hg ($R = 1.287$). The Hg recovery rate (93%) from Hg-loaded kaolinite at 1 mg/L Hg was higher compared to 22% from 1 mg/L Hg. Kaolinite can serve as a carrier to enhance Hg transport in porous media, with 250 mg/L kaolinite mobilizing ~2.4% Hg presorbed onto sand media. Correlation analysis revealed that desorbed Hg was significantly correlated with kaolinite ($r = 0.81$, $P < 0.0001$). Hence kaolinite enhanced Hg transport in the sand media serving both as a carrier (Hg was loaded before transport) and as mobile colloids stripping Hg off the sand media (Hg was loaded during transport).

Published by Elsevier B.V.

1. Introduction

Over the last decade, nano-particles and colloids from soils, mine wastes and industrial products have attracted an increasing interest due to their high affinity to contaminants and risks to human health [1–4]. Mathematical models based on advection–dispersion with flow and retention-release in surrounding media have been developed to describe the fate and transport of nano-particles and colloids in porous media [5,6].

Among heavy metals, Hg is of the most concern as it is highly toxic to living organisms including humans and animals. Due to atmospheric deposition caused by their proximity to industrial plants, surface soils have elevated Hg levels [7–10]. In addition, Hg is also present in high quantity in reservoir sediments and downstream floodplain soils due to transport process [11]. As a highly particle-reactive metal, Hg is mainly associated with fine particles in soil, including clay minerals, Fe/Mn oxides, and organic matter [12,13].

Hence, colloids play an important role in controlling Hg partitioning in soil and water system. Studies showed that a large proportion of mobile Hg was associated with colloids [14,15]. In Florida Everglades, for example, colloidal Hg comprises the majority of mobile Hg with only 10% being in dissolved forms (<3 kDa) [15]. In some rivers in the US, colloidal Hg comprised up to 72% of total Hg [14]. Both colloidal and dissolved Hg can be toxic to aquatic organisms [16].

Kaolinite [$Al_2Si_2O_5(OH)_4$] is a common clay mineral in soils of tropical region. Colloidal kaolinite in soils is mobile and can facilitate the transport of heavy metals [17,18]. Its mobility is affected by various geochemical parameters, e.g., flow rate, void fraction, ionic strength, and pH [19]. In addition, it also depends on colloid sorption capacity of the metal [20,21]. The maximum sorption capacity of kaolinite for Hg ranges from 0.12 to 1.3 mg/g [22]. Colloidal stability is also important for its transport behavior in soil. In the soil environment, kaolinite particles are often negatively charged, aggregates easily under acidic conditions and at low ionic strength [23]. Sorption of heavy metals onto colloids alters its surface charge. For example, addition of Cu, Pb, and Ca increases the aggregation rates of humic-coated kaolinite particles [24,25], hence increasing their deposition rate. However, the effect of Hg^{2+} on kaolinite colloid stability and mobility has not been well examined.

* Corresponding author.
E-mail address: lqma@ufl.edu (L.Q. Ma).

0304-3894/$ – see front matter. Published by Elsevier B.V.
doi:10.1016/j.jhazmat.2012.01.061

Several studies demonstrated in situ mobilization and transport of colloidal Hg from mine waste [26–28]. The colloidal Hg from mining wastes accounts for 95% of the total Hg during episodic particle release. The Hg-bearing colloids (10–200 nm) contain hematite, jarosite/alunite, and Al–Si gel [26]. Most studies on the release mechanisms of in situ Hg-bearing colloids focus on colloid mobilization induced by changing chemical conditions. However, limited research examined the ability of mobile colloids to desorb Hg, which has been presorbed to porous media. We hypothesize that mobile kaolinite colloids can compete with stationary Hg-bearing sand media. The high Hg sorption capacity of kaolinite can stripe Hg from sand and form kaolinite–Hg complex, thus facilitating Hg transport.

The objective of this study were to (1) determine the transport of kaolinite and Hg in saturated sand media; (2) investigate the transport of soluble Hg + kaolinite mixture under different Hg concentrations; (3) compare the effects of preloading Hg onto kaolinite on kaolinite and Hg transport in saturated sand media; and (4) test the ability of kaolinite to mobilize Hg from Hg-loaded sand media. Batch isotherm and column breakthrough experiments and mathematical model were used to fulfill these objectives.

2. Materials and methods

2.1. Characterization of sand and kaolinite

Quartz sand was used as the porous medium (Standard Sand & Silica Co.) in the batch and column experiments. The sand was sieved to ~0.55 mm, washed with 0.1 M NaOH, 1 M HNO_3 and deionized (DI) water, and then heated in a muffle furnace (Fisher Scientific, USA) at 550 °C to remove trace organic impurities and Fe/Al oxides. The sand was mainly composed of quartz and amorphous silica (>99%) based on X-ray diffraction analysis (Ultima IV multipurpose X-ray diffraction system, Rigaku, USA). After washing, the sand still contained 21 and 751 mg/kg Fe and Al (data not shown). The cation exchange capacity (CEC) of the sand and kaolinite were 6 and 84 mmol/kg, respectively. The zeta potential of kaolinite and Hg-loaded kaolinite was measured using Zeta Plus (Brookhaven instrument corporation, USA) (Table 1). The point of zero charge (PZC) of sand and kaolinite were 5.56 and 4.42 determined by potentiometry titration method [29] (Table 1).

The colloidal kaolinite was prepared according to the procedure of Sun et al. [30]. 5.0 g of kaolinite was suspended in 1 L DI water. The suspension was shaken vigorously, placed in an ultrasonic bath for 30 min, and then sit for 24 h. The fraction of kaolinite remaining in suspension after 24 h was siphoned into a second flask. The concentration of kaolinite in this suspension was determined gravimetrically before diluting an aliquot of the stock to proper colloid concentration. The mean size of the kaolinite colloids, as determined by photon correlation spectroscopy, was ~1.02 μm and did not vary significantly during the experiments (Table 1).

2.2. Batch experiments

Batch experiments were conducted to study Hg sorption onto kaolinite and sand. Each vessel was filled with a predetermined amount of sorbent (~2.5 g kaolinite or 5.0 g sand) and 50 mL of solutions (0, 0.5, 2.5, 5.0, 10, 25, 75, and 100 mg/L Hg) at pH 6 ± 0.2. The vessels were shaken on an end-over-end shaker for 48 h and centrifuged for 1 h at 2850 × *g*. Preliminary kinetic studies indicated 48 h was enough to achieve equilibrium. Aliquots of supernatant were acidified to determine total Hg concentrations using inductively coupled plasma–atomic emission spectroscopy (ICP-AES, detection limit = 0.01 mg/L) for high Hg concentration and hydride generation atomic fluorescence spectrometry (HGAFS, detection limit = 2 ng/L) for low Hg concentration. Hg concentrations in the solid phase were obtained via mass balance.

The stability of 50 mg/L kaolinite colloids under different Hg concentrations (1–100 mg/L, pH was 6) was estimated by optical density measurement. The kaolinite–Hg suspension was determined by UV–visible spectroscopy (Shimadzu, Japan) at 350 nm after sitting for 20 h.

2.3. Column experiments

Column experiments were conducted in 2.5 cm (diameter) × 15 (length) glass chromatography column (Kontes®). To make saturated porous media, the quartz sand was wet-packed in the column according to Chen et al. [31]. Approximately 125 g of sand was used to pack one column with a porosity of 0.42 and a pore volume (PV) of 32.5 mL. A peristaltic pump was connected to the inlet at the top of the column to regulate the downward flow of water and solutions at a constant rate of 1 mL/min. DI water was first pumped through the saturated column for ~2 h to remove impurities followed by working solutions. Samples at the column outlet were collected by an automatic fraction collector in glass vials for colloid analysis by UV/VIS at 350 nm and analyzed for Hg by HGAFS after acidification. The input solution pH was adjusted to 6 ± 0.2.

Two colloid suspensions were introduced to the sand column for colloid breakthrough studies, 100 mg/L kaolinite (Exp. 1; Table 2) and 100 mg/L Hg-loaded kaolinite (Exp. 6 and 7; Table 2). The colloid suspension was applied to the column as a 1 h pulse (2 PV), and then the column was flushed with DI water for 2 h. The Hg-loaded kaolinite suspension was prepared by mixing 25 mL of 1000 mg/L kaolinite suspension with 25 mL of 1 or 100 mg/L $Hg(NO_3)_2$ (Fisher Scientific, Pittsburgh). After being shaken on an end-over-end shaker for 24 h, the mixture was centrifuged to separate the solids from the liquid phase. The supernatant was then carefully withdrawn and 50 mL DI water was used to re-suspend the solid phase in ultrasonic bath for 30 min. The kaolinite suspension was washed twice with 50 mL DI water. The final suspension was then stored as a stock solution of Hg-loaded kaolinite, with the Hg concentration on kaolinite being 73 and 430 mg/kg for 1 and 100 mg/L Hg treatment (Table 2). For all experiments, $Hg(NO_3)_2$ was used to prepare Hg solution.

The Hg transport experiment was divided into two stages. To study the Hg transport behavior, Hg was added at two concentrations: 1 and 100 mg/L, which corresponded to low concentration found in contaminated water and high concentration to saturate the sand column with Hg. Hg solution was injected into the sand column as a 3 h pulse followed by 3 h flushing with DI water at Stage 1 (Exp. 2 and 3; Table 2). The sand in the column with sorbed Hg will be referred to as Hg-loaded sand, which contained 1.04 and 3.60 mg/kg Hg (Table 2). To investigate the ability of kaolinite in mobilizing Hg from Hg-loaded sand, the column was first flushed with DI for 6 h, then kaolinite suspension at 250 mg/L was introduced to the columns for 1 h followed by 2 h DI water flushing at Stage 2 (Exp. 8 and 9; Table 2). To study the interactions of kaolinite and Hg during their transport, solution containing 1 or 100 mg/L Hg was mixed with 100 mg/L kaolinite for 24 h. The amount of Hg sorbed onto kaolinite was 1018 and 1273 mg/kg for the two Hg concentrations (Table 2). The suspension, which contained soluble Hg and Hg sorbed onto kaolinite, was then introduced to sand column for 3 h followed by 3 h DI water flushing (Exp. 4 and 5; Table 2). Effluent samples for all experiments were collected from the bottom of the column with a fraction collector, and effluent from Exp. 4 and 5 were digested by concentrated HNO_3 at 110 °C.

Bromide was applied to the column as a conservative tracer for the breakthrough studies. The experiment procedures were the same as those used for colloid suspension. An ion chromatograph

Table 1
Selected properties of kaolinite colloids and sand porous media.

Material	Particle size (μm)	PZC[a]	CEC[a] (mmol/kg)	Zeta potential (mv)
Sand	550 ± 50	5.56 ± 0.31	6.0 ± 0.6	–
Kaolinite	1.02 ± 0.14	4.42 ± 0.22	84 ± 2.7	−17.2 ± 0.3
Hg_1-loaded kaolinite[a]	0.95 ± 0.21	–	–	−14.3 ± 0.4
Hg_{100}-loaded kaolinite[a]	1.05 ± 0.23	–	–	−11.1 ± 0.5

[a] PZC, point of zero charge; CEC, cation exchange capacity; Hg-loaded kaolinite was produced by mixing 1000 mg/L kaolinite with 1 or 100 mg/L Hg for 24 h after removing soluble Hg, resulting in 73 and 430 mg Hg/kg kaolinite.

(ICS-90, Dionex Corporation) was used to determine bromide concentrations.

2.4. Mathematic modeling

The Langmuir model was used to describe the sorption isotherms of Hg onto the sand and kaolinite:

$$X = \frac{KX_m C_e}{1 + KC_e} \quad (1)$$

where X is the Hg concentration on the solid phase (mg/g); X_m denotes the Langmuir maximum capacity (mg/g); K is a constant related to the binding strength of Hg ($L\,mg^{-1}$); and C_e is the Hg concentration in the solution (mg/L).

One dimension advection–dispersion equation coupled with reaction terms was used to simulate the transport of colloids or Hg in water-saturated sand column. The governing equations can be written as:

$$R\frac{\partial C_w}{\partial t} + \frac{\rho_b}{\theta_s}\frac{\partial C_s}{\partial t} = D\frac{\partial^2 C_w}{\partial x^2} - v\frac{\partial C_w}{\partial x} \quad (2)$$

$$\frac{\rho_b}{\theta_s}\frac{\partial C_s}{\partial t} = kC_w \quad (3)$$

where C_w represents concentration of colloid or Hg in pore water (mg/L); C_s is the concentration retained by the sand grain (mg/g); R is the retardation factor; ρ_b is sand bulk density ($g\,dm^{-3}$); θ_s is the saturated moisture content; D is the dispersion coefficient ($cm^2\,min^{-1}$); v is the velocity of pore water (cm/min); and k is the first-order rate constant (min^{-1}), which reflects irreversible, kinetic deposition of colloids or Hg onto grain surfaces.

The governing equations for the transport model were solved numerically for a zero initial concentration, a pulse-input boundary condition at the column inlet, and a zero-concentration-gradient boundary condition at the outlet. The model was first applied to bromide breakthrough data to estimate the dispersion coefficient D, which was used for the D of colloids and Hg. We assumed that the D of colloids and Hg is the same as that of the bromide tracer in the column. The model fitted parameters of Hg and kaolinite transport in columns were then quantified by the best-fit values of R^2.

2.5. Statistical analyses

Triplicate samples were used in batch experiments and duplicate samples were used in column experiments. All correlation and regression tests were performed using SAS 9.2 software. Level of significance for all tests were at $\alpha = 0.05$.

3. Results and discussion

3.1. Hg sorption isotherms onto sand and kaolinite

Hg sorption onto sand and kaolinite was nonlinear and fit to the Langmuir model ($R^2 = 0.99$ and 0.98; Fig. 1). The Langmuir model assumes uniform sorption energy onto the surface and little Hg transmigration on the surface plane [32]. The observed nonlinear sorption behavior indicated that Hg uptake onto sand or kaolinite occurred on a homogeneous surface via monolayer sorption with little interaction between sorbed Hg.

The maximum Hg sorption capacity on kaolinite (1.2 mg/g) was 11 times greater than that of sand (0.11 mg/g), which was consist with the larger surface area and higher CEC of kaolinite (Table 1) [14,33]. The maximum Hg sorption of kaolinite was similar to the reported 1.3 mg/g [34]. Based on the MINTEQ chemical equilibrium model, at our experimental conditions at pH 6, Hg^{2+} existed

Table 2
Parameters of kaolinite and Hg transport in saturated sand columns.

Exp. #	Solute or colloids	Hg on kaolinite or sand (mg/kg)	Recovery%* Hg/kaolinite	Max C/C_0* Hg/kaolinite	PV* Hg/kaolinite	R*	k (min^{-1})*	R^2*
	Bromide	–	–	–	–	1	0	
1	100 mg/L kaolinite (K_{100})	–	–/93	–/0.94	–/1.2	1	0.0019	0.98
2[a]	1 mg/L Hg (Hg_1)	–	22/–	0.40/–	6.1/–	–	–	–
3[b]	100 mg/L Hg (Hg_{100})	–	97/–	0.90/–	3.9/–	1.29	0.0023	0.96
4[a]	1 mg/L Hg + 100 mg/L kaolinite (Hg_1 + K_{100})	1018	13/5	0.24/0.99	7.0/6.6	–	–	–
5[b]	100 mg/L Hg + 100 mg/L kaolinite (Hg_{100} + K_{100})	1273	90/18	1.00/0.84	6.1/6.6	1.35	0.0025	0.95
6	100 mg/L Hg_1-loaded kaolinite (Hg_1-loaded K_{100})[c]	73.0	93/93	0.92/0.92	1.2/1.2	1	0.0030	0.98
7	100 mg/L Hg_{100}-loaded kaolinite (Hg_{100}-loaded K_{100})[c]	430	78/78	0.76/0.76	1.5/1.5	1	0.0090	0.98
8	250 mg/L kaolinite (K_{250})/Hg_1-loaded sand[d]	1.04	–/97	–/0.95	1.5/1.5	1	0.0032	0.98
9	250 mg/L kaolinite (K_{250})/Hg_{100}-loaded sand[d]	3.60	–/92	–/0.94	1.2/1.2	1	0.0034	0.97

[a] The data in Exp. 2 and 4 could not be fit by the model.
[b] Model fitted parameters R and k in Exp. 3 and 5 were for Hg, and the rest were for kaolinite.
[c] They were prepared by mixing 1000 mg/L kaolinite with 1 or 100 mg/L Hg for 24 h after removing soluble Hg.
[d] Hg-loaded sand was from Exp. 2 and 3 where the sand media were leached with 1 or 100 mg/L Hg.
* C/C_0, relative concentration, PV, pore volume at maximum C/C_0, R, retardation factor, k, kinetic reaction rate constant, and R^2, correlation between model and experimental data.

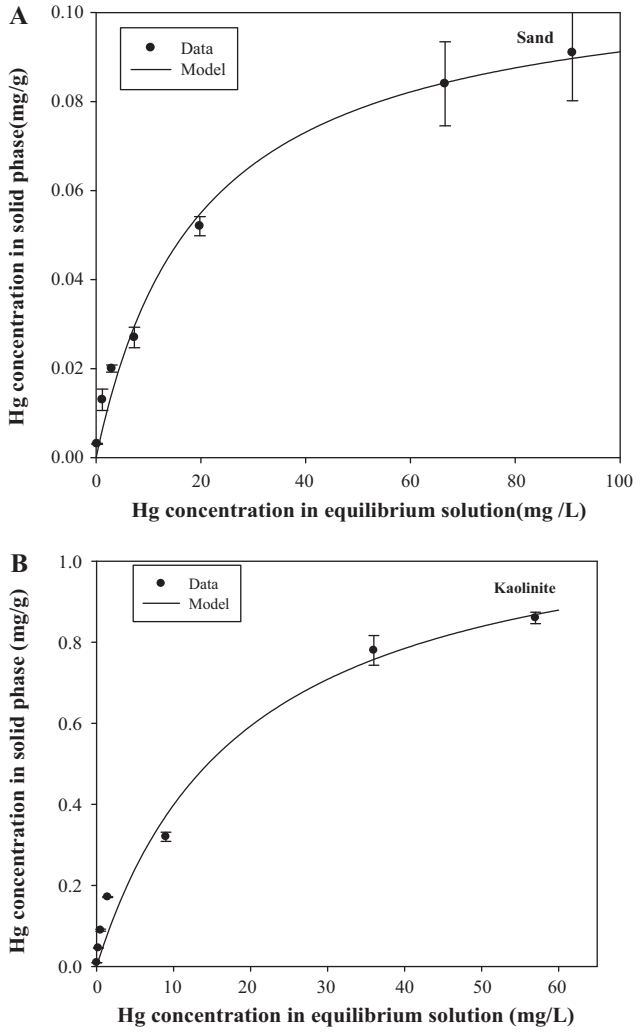

Fig. 1. Sorption isotherms of Hg onto sand and kaolinite after 48 h of reaction.

predominately as neutral species $Hg(OH)_2^0$ (~99%). Sarkar et al. [35] also reported that $Hg(OH)_2^0$ is the predominant solution species at >pH 5. For both sand (contained 756 mg/kg Al) and kaolinite, surface functional groups XOH (X = Al or Si) may be responsible for Hg sorption via formation of XO—$HgOH^+$ species [35].

Based on the Langmuir model, the Hg binding constant K for sand and kaolinite were 0.049 and 0.053 L mg^{-1} (data not shown). The data suggest that the sand had lower binding strength than kaolinite. The slightly higher Hg sorption affinity by kaolinite may enable kaolinite to desorb Hg from sand surface.

3.2. Kaolinite and Hg transport in saturated sand column

Transport of 100 mg/L kaolinite (K_{100}), and 1 and 100 mg/L Hg (Hg_1 and Hg_{100}) was performed in saturated sand column (Exp. 1–3; Table 2). Based on the breakthrough curve (BTC), at low ionic strength (DI water), K_{100} transport was similar to that of conservative tracer bromide (data not shown), indicating that kaolinite deposition rate onto sand media was low (Fig. 2A). However, relative kaolinite concentration (C/C_0) did not exceed 0.94 (Table 2), suggesting that small amount (~7%) of kaolinite was retained on sand grains. Similar phenomenon was observed in illite and montmorillonite transport in sand media [36].

Different from kaolinite, Hg transport at both concentrations showed a sharp sorption front with a substantial tailing of desorption front (Fig. 2B). The Hg transport through the sand columns was

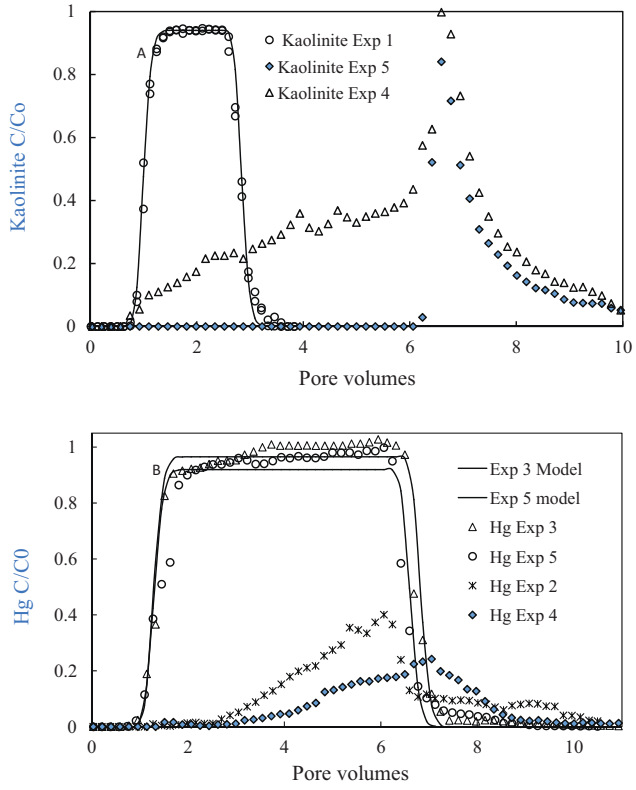

Fig. 2. Breakthrough curves (BTC) in water-saturated sand column: (A) kaolinite BTC at 100 mg/L kaolinite with 0 (Exp. 1), 1 (Exp. 4) or 100 mg/L Hg (Exp. 5), and (B) Hg BTC at 1 mg/L Hg with 0 (Exp. 2) or 100 mg/L kaolinite (Exp. 4), or 100 mg/L Hg with 0 (Exp. 3) or 100 mg/L kaolinite (Exp. 5) (Table 2).

retarded significantly more than kaolinite transport. The maximum C/C_0 of kaolinite was at 1.2 PV (pore volume; Fig. 2A) compared to 3.9 PV (C_0 = 100 mg/L Hg) and 6.1 PV (C_0 = 1 mg/L Hg) for Hg (Fig. 2B). The delayed transport and tailing of Hg desorption front suggested Hg sorption onto the sand grains. At 1 mg/L Hg (Exp. 2; Table 2), large amount of Hg (22%) was sorbed onto the sand column with low C/C_0 at 0.4. In this case, sorption sites on sand were not saturated with Hg, with 0.13 mg Hg being sorbed onto 125 g of sands (1.04 mg/kg). At 100 mg/L Hg (Exp. 3; Table 2), relative Hg concentration C/C_0 in the effluent was 0.90 at 0.96 PV, then slowly reaching equilibrium (C/C_0 = 1) at 3.9 PV. The data indicated that introducing 100 mg/L Hg for 3 h (5.4 PV) was sufficient to reach a steady state with Hg sorption onto sand. Mass balance calculation showed that 0.45 mg Hg was sorbed onto 125 g of sands, with Hg concentration reaching 3.60 mg/kg, which was much smaller than its maximum sorption capacity of 110 mg/kg based on batch experiment (Fig. 1). This observation indicated that sorption data via batch experiment at equilibrium could not be applied to predict Hg breakthroughs in column experiment. Hg retention onto sand column was also reported by Liao et al. [42]. After introducing 8 mg/L Hg to saturated sand media, the peak of BTC did not exceed 2 mg/L Hg with only 17% of the Hg recovered in the leachate. Their data again suggest substantial Hg sorption onto sand grain surfaces.

The one dimension advection and dispersion transport model was applied to stimulate transport behavior of kaolinite and Hg in saturated sand column. For the stimulations, the colloid dispersion coefficient D was determined based on Br^- tracer experiment (data not shown). The estimated D at 0.047 cm^2 min^{-1} was similar to the reported values [30,37]. Best fit first-order rate constant k for kaolinite and Hg transport were determined by Leverberg–Marquadi algorithm method. The model revealed most features of BTCs for transport

of K_{100} and Hg_{100} (Exp. 1 and 3). The model simulations matched well with the experimental BTCs of Hg and kaolinite with R^2 of 0.96–0.98 (Fig. 2 and Table 2). For K_{100} and Hg_{100}, the retardation factor (R) was 1 and 1.29, and deposition rate (k) was 0.0019 and 0.022 (min^{-1}) (Table 2). The higher R and k values for Hg transport than kaolinite transport suggested stronger interactions between Hg and sand media (Fig. 2B). However, the same model cannot fit the Hg_1 transport data (Exp. 2), indicating that non chemical equilibrium or non linear sorption condition existed for Hg transport in sand column at 1 mg/L Hg.

3.3. Hg and kaolinite interactions during transport

To determine the interactions of Hg and kaolinite during the transport, the transport of Hg_{100} (Exp. 3) was compared to that of $Hg_{100} + K_{100}$ (Exp. 5). In $Hg_{100} + K_{100}$, the Hg concentration on kaolinite was 1.3 mg/g (Table 2). Given the maximum Hg sorption capacity of kaolinite at 1.2 mg/g based on Langmuir model (Fig. 1), kaolinite was oversaturated with Hg, with soluble Hg dominating the $Hg_{100} + K_{100}$ mixture. The effluent Hg concentrations were slightly lower in $Hg_{100} + K_{100}$ transport (99.2 mg/L) than in Hg_{100} transport (Fig. 2B). The recovery for total Hg was 97% in Hg_{100} transport, which was significantly higher than that of $Hg_{100} + K_{100}$ transport (90%) (Table 2). From model calculation, the best fitting R and k for Hg in $Hg_{100} + K_{100}$ transport was 1.35 and 0.0025, which were higher than those in Hg_{100} transport (1.29 and 0.0023) (Table 2). These observations showed that co-injecting soluble Hg with kaolinite decreased Hg's mobility compared to Hg transport. From the kaolinite BTC in $Hg_{100} + K_{100}$ transport (Exp. 5; Fig. 2A), higher retardation of kaolinite transport was observed. The maximum C/C_0 of kaolinite was detected at 6.6 PV in $Hg_{100} + K_{100}$ transport, which was much later than that of K_{100} transport at 1.2 PV (Table 2). Kaolinite recovery in $Hg_{100} + K_{100}$ transport (18%) was much lower than that of K_{100} transport (93%). These results demonstrated that soluble Hg increased irreversible deposition of kaolinite colloids ($k = 0.0025$). Similarly, Tang and Weisbrod [38] found that montmorillonite suspension at 100 mg/L was destabilized by soluble Pb at 16–30 mg/L during its transport in discrete fractures, with the maximum C/C_0 being reduced by 38–39%. The increased colloid deposition onto sand also explained the elevated retention of soluble Hg on sand surface. This was because kaolinite had higher sorption capacity for Hg than sand, adding kaolinite to sand surface led to the higher Hg sorption onto sand. Comparison of Hg and kaolinite BTC in $Hg_{100} + K_{100}$ transport, the total Hg concentration did not co-vary with kaolinite concentration. This was because, in the $Hg_{100} + K_{100}$ mixture, Hg was not mainly associated with kaolinite, with >99% Hg being soluble Hg (99.2 mg/L).

In natural systems, aqueous Hg concentrations in groundwater and surface water are commonly < 30 ng/L [39]. However, in highly polluted waters, Hg concentration can reach 2 mg/L [11]. To further understand the interaction of Hg with kaolinite, we studied the transport of $Hg_1 + K_{100}$ (Exp. 4, Table 2). In this Hg and kaolinite mixture, Hg concentration on kaolinite was 1.02 mg/g, making Hg sorbed on kaolinite account for ~10% of total Hg. Similar to transport of $Hg_{100} + K_{100}$, the BTCs of $Hg_1 + K_{100}$ transport (Exp. 4) showed higher retardation and deposition rate compared to K_{100} (Exp. 1) and Hg_1 transport (Exp. 2) (Fig. 2). The maximum C/C_0 of Hg was 0.24 (Exp. 4; Fig. 2B, Table 2), which was lower than that of 0.4 for Hg_1 transport (Exp. 2, Fig. 2B). The maximum C/C_0 of kaolinite was detected at 6.6 PV (Exp. 4), which was also later than that of K_{100} at 1.2 PV (Exp. 1, Table 2). The recovery for total Hg (13%) in $Hg_1 + K_{100}$ transport (Exp. 4, Table 2) was significantly lower than that in Hg_1 transport (22%) (Exp. 2, Table 2). Pearson correlation analysis showed that total Hg concentration was significantly correlated with kaolinite ($r = 0.88$, $P < 0.0001$) (data not shown). In this situation, Hg transport was more correlated with kaolinite

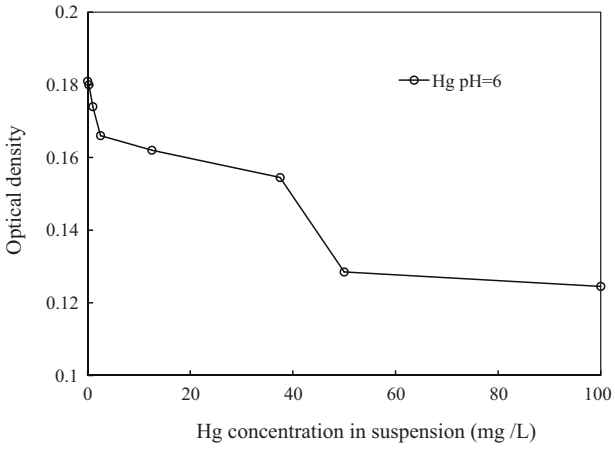

Fig. 3. Influence of Hg concentration on the stability of kaolinite colloids.

transport though colloidal Hg accounted for only 10% (0.11 mg/L) of total Hg. Such discrepancies between colloidal Hg transport behavior at low and high Hg systems have been observed for Cs^+ colloid transport. At the low Cs loading, high percentage of Cs was retained on the colloids, leading to colloid-facilitated Cs transport. When Cs concentration increased to a sufficiently high level to saturate the high affinity sites of both colloids and collector grains, Cs transport in soluble phase dominates the breakthrough process [40].

The column experiment results were consisted with batch experiment (Fig. 3), both confirmed that the presence of Hg decreased kaolinite stability and higher Hg concentration led to higher rate of kaolinite aggregation (Figs. 2 and 3). It can be explained that the increase in divalent cations concentration increases positive charge on colloids surface, reducing electrostatic repulsion and leading to colloids aggregation [23,41].

3.4. Transport of Hg-loaded kaolinite

The effect of Hg on kaolinite transport was further evaluated by preloading Hg (1 or 100 mg/L) onto 100 mg/L kaolinite (Hg_1-loaded and Hg_{100}-loaded kaolinite), with Hg concentration on kaolinite at 0.073 and 0.43 mg/g (Table 2). While both soluble Hg and kaolinite co-existed in $Hg_{100} + K_{100}$ transport in Exp. 4 and 5, there was no soluble Hg in Hg-loaded kaolinite in Exp. 6 and 7 as they were removed. Hg on Hg_1-loaded K_{100} accounted for 6.6% of its maximum sorption capacity (Exp. 6, Table 2). At this Hg loading, Hg did not impact kaolinite's transport much (Fig. 4). The kaolinite recovery from Hg_1-loaded K_{100} and K_{100} was similar at ~93% (Exp. 6 and 1, Table 2).

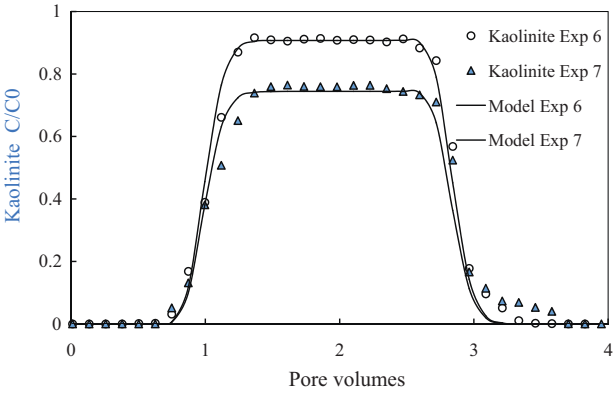

Fig. 4. Impact of preloading Hg (1 or 100 mg/L Hg) onto 100 mg/L kaolinite on kaolinite transport in sand column: (Exp. 6 and 7, Table 2).

Compared to Hg_1-loaded K_{100}, preloading 100 mg/L Hg onto kaolinite had greater impact on kaolinite transport. The Hg_{100}-loaded K_{100} (Exp. 7; Table 2) showed a lower C/C_0 (0.76) and recovery (78%) compared to 0.94 and 93% from K_{100} transport (Fig. 2A, Exp. 1, Table 2). Based on the transport model, the k was 0.0090 in Hg_{100}-loaded K_{100}, which was three times greater than those of K_{100} and Hg_1-loaded K_{100} transport (0.0030; Table 2). The results indicated higher deposition rate of Hg_{100}-loaded K_{100} on sand media than K_{100}. The model described the BTC of Hg-loaded K_{100} well with R^2 of 0.94–0.97 (Fig. 4, Table 2). This was confirmed by the changes in zeta potential of Hg-loaded kaolinite. As Hg loading increased from 0.073 to 0.43 mg/g, its zeta potential increased from −14.3 to −11.1 mV (Table 1). The particle size was 0.95 and 1.1 μm for Hg_1-loaded and Hg_{100}-loaded kaolinite (Table 1). No significant difference in particle size was found compared to kaolinite (1.0 μm).

In addition to the effect of Hg on kaolinite mobility, the transport of Hg-loaded kaolinite (carrying both Hg and kaolinite) also reflected the effect of kaolinite on Hg transport as a carrier. During the transport, no detectable Hg release was found in Hg-loaded kaolinite suspension, so Hg retardation factor and recovery rate were the same as kaolinite. Hg retardation ($R = 1$) in Hg_{100}-loaded kaolinite transport was much lower compared to that from Hg_{100} transport ($R = 1.29$). The results indicated Hg transported faster when loaded onto kaolinite, i.e., kaolinite facilitated Hg transport in the sand media as a carrier. In addition, the Hg recovery rate from Hg_1-loaded kaolinite (Exp. 4, Table 2) was 93% (assuming same recovery rate as kaolinite, i.e., no Hg release during the transport process) compared to 22% from Hg_1 transport (Exp. 2, Table 2) from the sand media (Fig. 2B). These evidences confirmed that kaolinite can serve as a carrier to enhance Hg transport in porous media.

3.5. Kaolinite mobilized Hg presorbed on sand media

To further demonstrate kaolinite-facilitated Hg transport, a higher concentration at 250 mg/L kaolinite (K_{250}) was injected into the sand media (Exp. 8 and 9, Table 2), which was preloaded with 1 or 100 mg/L Hg (Hg_1-loaded and Hg_{100}-loaded sand, Exp. 2 and 3, Table 2). Both kaolinite and Hg concentrations showed a peak within 1.5 PV (Fig. 5), indicating that kaolinite scavenged Hg presorbed onto the sand media. This observation is consistent with other reports regarding Hg adsorption and desorption. Both irreversible and slowly reversible process was the dominant mechanism for Hg sorption in sand. For Hg-loaded sand, the amount of Hg desorbed increased from 0.003 mg in Hg_1-loaded sand to 0.01 mg in Hg_{100}-loaded sand. The significant Hg desorption from Hg_{100}-loaded sand may indicate that most of the Hg was sorbed onto low-energy sites and can be easily desorbed [42]. In the early stage of Hg desorption (1–2 PV), the Hg concentration had strong positive correlation with kaolinite (Fig. 5), i.e., Hg concentration increased as kaolinite concentration increased. The higher affinity of kaolinite for Hg over sand resulted in Hg to be stripped from the sand and sorbed onto the migrating kaolinite (binding constant $K = 0.053$ and 0.049 L mg^{-1} for kaolinite and sand). In the later transport stage, kaolinite concentration was more stable, whereas Hg concentration showed decreasing trend for both Hg-loaded sand (Fig. 5). This can be explained by the limited exchangeable Hg on sand sites. Pearson correlation analysis showed that effluent Hg concentration was significantly correlated with kaolinite ($r = 0.811$ and 0.807, $P < 0.0001$) (data not shown), thereby the extent of Hg mobilization from the sand media was strongly affected by injected kaolinite. Similar trends in Hg mobilization by kaolinite were observed in Hg_1-loaded sand and Hg_{100}-loaded sand. Sun et al. [30,43] demonstrated that mobile kaolinite scavenged the presorbed Pb from the sand surface to facilitate Pb transport, and kaolinite and Pb concentration in effluents showed a strong linear relationship. Bartona

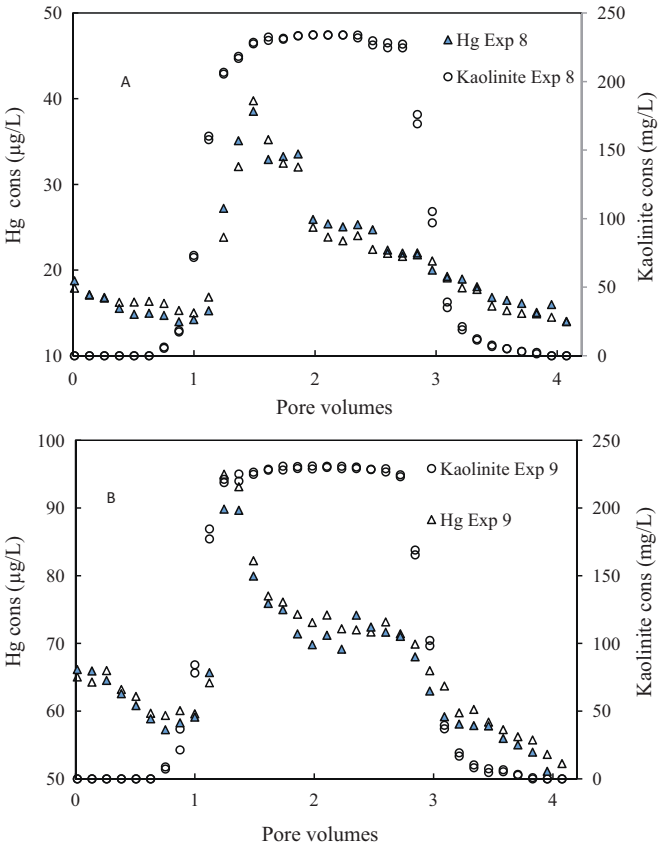

Fig. 5. Breakthrough curves of Hg and 250 mg/L kaolinite in sand column, which were preleached with 1 mg/L Hg (A) and 100 mg/L Hg (B) for 2 h (Exp. 8 and 9, Table 2).

and Karathanasis [43] reported Zn desorption from contaminated soil onto ex situ mobile mineral colloids, which had high sorption affinity for Zn and small particle diameter (<0.8 μm). The colloids showed considerable migrating ability through the soil matrix and enhanced Zn desorption by up to 400 times over that exhibited by DI water. Statistical analysis of effluent Hg concentration from the two Hg-load sand media showed significant difference ($p < 0.001$), with Hg_{100}-loaded sand media having more Hg mobilized than Hg_1-loaded sand. Mass balance calculations showed that kaolinite mobilized 2.5% and 2.4% retained Hg from the Hg_1-loaded and Hg_{100}-loaded sand media (Fig. 5). These data showed that 250 mg/L kaolinite was sufficient to stripe Hg presorbed onto sand surfaces.

4. Conclusions

Both batch sorption experiment and column transport experiment showed that kaolinite had higher sorption capacity and binding strength than sand for Hg. During $Hg_{100} + K_{100}$ transport, both the mobility of kaolinite and Hg were reduced, with low recovery rate and high retardation. Soluble Hg dominated the $Hg_{100} + K_{100}$ transport whereas colloidal Hg (Hg associated with kaolinite) impacted the $Hg_1 + K_{100}$ transport. Though preloading kaolinite with high Hg (0.43 mg/g) reduced kaolinite's mobility with relative low BTCs recovery (78%) in transport of Hg_{100}-loaded kaolinite, still kaolinite served as a carrier to enhance Hg transport in sand media. This is because Hg retardation ($R = 1$) in Hg_{100}-loaded kaolinite was much lower compared to retardation of Hg_{100} ($R = 1.29$). In addition, the Hg recovery rate (93%) from Hg_1-loaded kaolinite was higher than that in Hg_1 transport (22%). In addition, Hg presorbed onto the sand media was mobilized and co-transported with mobile kaolinite, with higher presorbed Hg

concentrations (100 vs. 1 mg/L Hg; Exp. 8 and 9, Table 2) resulting in higher Hg mobilization by mobile kaolinite (~2.4%). Hg mobilization and kaolinite concentration had significant positive correlation, indicating mobile kaolinite was responsible for Hg mobilization. Our research demonstrated that kaolinite enhanced Hg transport in the sand media serving both as a carrier when Hg was loaded before transport. In addition, kaolinite also can stripe Hg off the sand media when Hg was preloaded sand column during transport. However, when kaolinite was added to soluble Hg, kaolinite reduced Hg transport. The colloid-facilitated Hg transport and the stripping effect of Hg from sand column have important implications for risk assessments of Hg mobility in soil environment.

Acknowledgements

This research was supported by the University of Florida IFAS Innovation grant. We were grateful to Mr. Yuan Tian in Agricultural and Biological Engineering Department and Ms. Hao Chen in Soil and Water Science Department for their help with the column experiment setup.

References

[1] X. Hu, X. Chen, J. Shi, Y. Chen, Q. Lin, Particle-facilitated lead and arsenic transport in abandoned mine sites soil influenced by simulated acid rain, Chemosphere 71 (2008) 2091–2097.
[2] L.F.O. Silva, J.C. Hower, M. Izquierdo, X. Querol, Complex nanominerals and ultrafine particles assemblages in phosphogypsum of the fertilizer industry and implications on human exposure, Sci. Total Environ. 408 (2010) 5117–5122.
[3] J. Ribeiro, D. Flores, C.R. Ward, L.F.O. Silva, Identification of nanominerals and nanoparticles in burning coal waste piles from Portugal, Sci. Total Environ. 408 (2010) 6032–6041.
[4] S.-W. Jeong, S.-D. Kim, Aggregation and transport of copper oxide nanoparticles in porous media, J. Environ. Monit. 11 (2009) 1595–1600.
[5] N. Tufenkji, M. Elimelech, Correlation equation for predicting single-collector efficiency in physicochemical filtration in saturated porous media, Environ. Sci. Technol. 38 (2003) 529–536.
[6] J. Simunek, C. He, L. Pang, S.A. Bradford, Colloid-facilitated solute transport in variably saturated porous media: numerical model and experimental verification, Vadose Zone J. 5 (2006) 1035–1047.
[7] I.J. Kostova, J.C. Hower, M. Mastalerz, S.V. Vassilev, Mercury capture by selected Bulgarian fly ashes: influence of coal rank and fly ash carbon pore structure on capture efficiency, Appl. Geochem. 26 (2011) 18–27.
[8] E.G. Pacyna, J.M. Pacyna, K. Sundseth, J. Munthe, K. Kindbom, S. Wilson, F. Steenhuisen, P. Maxson, Global emission of mercury to the atmosphere from anthropogenic sources in 2005 and projections to 2020, Atmos. Environ. 44 (2010) 2487–2499.
[9] L. Silva, M. Izquierdo, X. Querol, R. Finkelman, M. Oliveira, M. Wollenschlager, M. Towler, R. Pérez-López, F. Macias, Leaching of potential hazardous elements of coal cleaning rejects, Environ. Monit. Assess. 175 (2011) 109–126.
[10] F. Goodarzi, F.E. Huggins, H. Sanei, Assessment of elements, speciation of As, Cr, Ni and emitted Hg for a Canadian power plant burning bituminous coal, Int. J. Coal Geol. 74 (2008) 1–12.
[11] A. Navarro, E. Cardellach, M. Corbella, Mercury mobility in mine waste from Hg-mining areas in Almería, Andalusia (Se Spain), J. Geochem. Explor. 101 (2009) 236–246.
[12] A. Bollen, A. Wenke, H. Biester, Mercury speciation analyses in $HgCl_2$-contaminated soils and groundwater – implications for risk assessment and remediation strategies, Water Res. 42 (2008) 91–100.
[13] G. Liu, J. Cabrera, M. Allen, Y. Cai, Mercury characterization in a soil sample collected nearby the DOE Oak ridge reservation utilizing sequential extraction and thermal desorption method, Sci. Total Environ. 369 (2006) 384–392.
[14] C.L. Babiarz, J.P. Hurley, S.R. Hoffmann, A.W. Andren, M.M. Shafer, D.E. Armstrong, Partitioning of total mercury and methylmercury to the colloidal phase in freshwaters, Environ. Sci. Technol. 35 (2001) 4773–4782.
[15] Y. Cai, R. Jaff, R.D. Jones, Interactions between dissolved organic carbon and mercury species in surface waters of the Florida Everglades, Appl. Geochem. 14 (1999) 395–407.
[16] J.-F. Pan, W.-X. Wang, Uptake Hg(II) and methylmercury by the green mussel Perna viridis under different organic carbon conditions, Mar. Ecol. 276 (2004) 125.
[17] M. Flury, J.B. Mathison, J.B. Harsh, In situ mobilization of colloids and transport of cesium in Hanford sediments, Environ. Sci. Technol. 36 (2002) 5335–5341.
[18] T. Cheng, J.E. Saiers, Mobilization and transport of in situ colloids during drainage and imbibition of partially saturated sediments, Water Resour. Res. 45 (2009) W08414.
[19] A. Tripathy, Hydrodynamically and chemically induced in situ kaolin particle release from porous media an experimental study, Adv. Powder Technol. 21 (2010) 564–572.
[20] P. Srivastava, B. Singh, M. Angove, Competitive adsorption behavior of heavy metals on kaolinite, J. Colloid Interface Sci. 290 (2005) 28–38.
[21] S. Sen Gupta, K.G. Bhattacharyya, Immobilization of Pb(II), Cd(II) and Ni(II) ions on kaolinite and montmorillonite surfaces from aqueous medium, J. Environ. Manage. 87 (2008) 46–58.
[22] Y. Aijun, Q. Changle, M. Shusen, E.J. Reardon, Effects of humus on the environmental activity of mineral-bound Hg: influence on Hg volatility, Appl. Geochem. 21 (2006) 446–454.
[23] R. Kretzschmar, H. Holthoff, H. Sticher, Influence of pH and humic acid on coagulation kinetics of kaolinite: a dynamic light scattering study, J. Colloid Interface Sci. 202 (1998) 95–103.
[24] R.A. Akbour, J. Douch, M. Hamdani, P. Schmitz, Transport of kaolinite colloids through quartz sand: influence of humic acid, Ca^{2+}, and trace metals, J. Colloid Interface Sci. 253 (2002) 1–8.
[25] I. Heidmann, I. Christl, R. Kretzschmar, Aggregation kinetics of kaolinite–fulvic acid colloids as affected by the sorption of Cu and Pb, Environ. Sci. Technol. 39 (2004) 807–813.
[26] G.V. Lowry, S. Shaw, C.S. Kim, J.J. Rytuba, G.E. Brown, Macroscopic and microscopic observations of particle-facilitated mercury transport from New Idria and sulphur bank mercury mine tailings, Environ. Sci. Technol. 38 (2004) 5101–5111.
[27] A.J. Slowey, S.B. Johnson, J.J. Rytuba, G.E. Brown, Role of organic acids in promoting colloidal transport of mercury from mine tailings, Environ. Sci. Technol. 39 (2005) 7869–7874.
[28] A.J. Slowey, J.J. Rytuba, G.E. Brown, Speciation of mercury and mode of transport from placer gold mine tailings, Environ. Sci. Technol. 39 (2005) 1547–1554.
[29] B. Van Raij, M. Peech, Electrochemical properties of some oxisols and alfisols of the tropics, Soil Sci. Soc. Am. J. 36 (1972) 587–593.
[30] H. Sun, B. Gao, Y. Tian, X. Yin, C. Yu, Y. Wang, L.Q. Ma, Kaolinite and lead in saturated porous media: facilitated and impeded transport, J. Environ. Eng. Sci. 136 (2010) 1305–1308.
[31] H. Chen, B. Gao, H. Li, L.Q. Ma, Effects of pH and ionic strength on sulfamethoxazole and ciprofloxacin transport in saturated porous media, J. Contam. Hydrol. 126 (2011) 29–36.
[32] X. Dong, L.Q. Ma, Y. Li, Characteristics and mechanisms of hexavalent chromium removal by biochar from sugar beet tailing, J. Hazard. Mater. 190 (2011) 909–915.
[33] M. Gabriel, D. Williamson, Principal biogeochemical factors affecting the speciation and transport of mercury through the terrestrial environment, Environ. Geochem. Health 26 (2004) 421–434.
[34] M. Arias, M.T. Barral, J. Da Silva-Carvalhal, J.C. Mejuto, D. Rubinos, Interaction of Hg(II) with kaolin–humic acid complexes, Clay Miner. 39 (2004) 35–45.
[35] D. Sarkar, M.E. Essington, K.C. Misra, Adsorption of mercury(II) by kaolinite, Soil Sci. Soc. Am. J. 64 (2000) 1968–1975.
[36] J.E. Saiers, Laboratory observations and mathematical modeling of colloid-facilitated contaminant transport in chemically heterogeneous systems, Water Resour. Res. 38 (2002) 1032.
[37] B. Gao, J.E. Saiers, J.N. Ryan, Deposition and mobilization of clay colloids in unsaturated porous media, Water Resour. Res. 40 (2004) W08602.
[38] X.-Y. Tang, N. Weisbrod, Colloid-facilitated transport of lead in natural discrete fractures, Environ. Pollut. 157 (2009) 2266–2274.
[39] J.L. Barringer, Z. Szabo, D. Schneider, W.D. Atkinson, R.A. Gallagher, Mercury in ground water, septage, leach-field effluent, and soils in residential areas, New Jersey coastal plain, Sci. Total Environ. 361 (2006) 144–162.
[40] J. Zhuang, M. Flury, Y. Jin, Colloid-facilitated Cs transport through water-saturated Hanford sediment and Ottawa sand, Environ. Sci. Technol. 37 (2003) 4905–4911.
[41] R. Kretzschmar, T. Schafer, Metal retention and transport on colloidal particles in the environment, Elements 1 (2005) 205–210.
[42] L. Liao, H.M. Selim, R.D. Delaune, Mercury adsorption–desorption and transport in soils, J. Environ. Qual. 38 (2009) 1608–1616.
[43] C.D. Bartona, A.D. Karathanasis, Colloid-enhanced desorption of zinc in soil monolith, Int. J. Environ. Stud. 60 (2003) 395–409.